



HAL
open science

AT-dependent luminescence of DNA-threading ruthenium complexes

Fredrik Westerlund, Per Lincoln

► **To cite this version:**

Fredrik Westerlund, Per Lincoln. AT-dependent luminescence of DNA-threading ruthenium complexes. *Biophysical Chemistry*, 2007, 129 (1), pp.11. 10.1016/j.bpc.2007.04.011 . hal-00501664

HAL Id: hal-00501664

<https://hal.science/hal-00501664>

Submitted on 12 Jul 2010

HAL is a multi-disciplinary open access archive for the deposit and dissemination of scientific research documents, whether they are published or not. The documents may come from teaching and research institutions in France or abroad, or from public or private research centers.

L'archive ouverte pluridisciplinaire **HAL**, est destinée au dépôt et à la diffusion de documents scientifiques de niveau recherche, publiés ou non, émanant des établissements d'enseignement et de recherche français ou étrangers, des laboratoires publics ou privés.

Accepted Manuscript

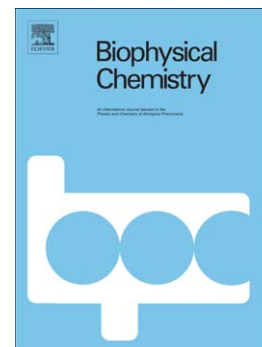
AT-dependent luminescence of DNA-threading ruthenium complexes

Fredrik Westerlund, Per Lincoln

PII: S0301-4622(07)00106-8
DOI: doi: [10.1016/j.bpc.2007.04.011](https://doi.org/10.1016/j.bpc.2007.04.011)
Reference: BIOCHE 4959

To appear in: *Biophysical Chemistry*

Received date: 3 April 2007
Accepted date: 25 April 2007



Please cite this article as: Fredrik Westerlund, Per Lincoln, AT-dependent luminescence of DNA-threading ruthenium complexes, *Biophysical Chemistry* (2007), doi: [10.1016/j.bpc.2007.04.011](https://doi.org/10.1016/j.bpc.2007.04.011)

This is a PDF file of an unedited manuscript that has been accepted for publication. As a service to our customers we are providing this early version of the manuscript. The manuscript will undergo copyediting, typesetting, and review of the resulting proof before it is published in its final form. Please note that during the production process errors may be discovered which could affect the content, and all legal disclaimers that apply to the journal pertain.

AT-Dependent Luminescence of DNA-Threading Ruthenium Complexes

Fredrik Westerlund^{#} and Per Lincoln*

Department of Chemical and Biological Engineering, Chalmers University of Technology,
SE-41296 Gothenburg, Sweden

^{*}email: fredrik.westerlund@chalmers.se

[#]Current address: Nano Science Center, University of Copenhagen, Dk-2100 Copenhagen,
Denmark. Tel: +45-353 21833

**RECEIVED DATE (to be automatically inserted after your manuscript is accepted if
required according to the journal that you are submitting your paper to)**

TITLE RUNNING HEAD: AT-Dependent Luminescence

Abstract

Whereas, the emission from the ruthenium complex $\Delta\Delta$ - $[\mu$ -bidppz(phen) $_4$ Ru $_2$] $^{4+}$ (**P**) is five times larger when intercalated into poly(dAdT) $_2$ than when intercalated into ct-DNA, the homologue $\Delta\Delta$ - $[\mu$ -bidppz(bipy) $_4$ Ru $_2$] $^{4+}$ (**B**) has a smaller quantum yield and a red-shifted emission. The origin of this difference is here investigated by studying intercalation into oligonucleotides containing a central AT-tract. Increasing the length of the AT-tract increases the emission quantum yield for **P** but decreases it for **B**. However, not even four helix turns of AT base pairs is enough to mimic poly(dAdT) $_2$. **B** and **P** thus use the increased flexibility with increasing length of the AT-tract in opposite ways, whereas **B** gets more prone to quenching by water, **P** gets more protected from quenching. The earlier reported gradual increase of the intercalation rate with AT-stretch length is thus paralleled by a gradual change in the equilibrium properties of the intercalated state.

KEYWORDS: “light switch”, binuclear ruthenium complex, DNA threading intercalation, luminescence

Introduction

Selective, non-covalent targeting of specific DNA-sequences by drug molecules is generally based on thermodynamically controlled equilibrium binding, which limits the selectivity to short sequences for moderately sized molecules. We have recently shown that a high selectivity for long stretches of alternating A-T base pairs can be attained through kinetically controlled DNA threading intercalation by binuclear ruthenium complexes, where the intercalation rate can vary by more than three orders of magnitude between mixed-sequence and alternating AT DNA.[1] The binuclear ruthenium complexes are of general formula $[\mu\text{-bidppz}(\text{L})_4\text{Ru}_2]^{2+}$ (bidppz=11,11'-bi(dipyrido-[3,2-*a*:2',3'-*c*]-phenaziny), L=1,10-phenanthroline (**P**) or L=2,2'-bipyridine (**B**), Figure 1), and bind to DNA by threading one of their bulky ruthenium centres through the DNA base stack. This results in an extremely slow binding process in which one Ru-centre ends up in each groove and the bridging bidppz ligand sandwiched between the base pairs.[2-5] Interestingly, for a series of oligonucleotide duplexes with a central AT-tract of varying length the intercalation rate shows a 100-fold increase when going from 10 to 20 consecutive AT base pairs, indicating that the transition state involves a stretch of AT base pairs considerably larger than the dimensions of the intercalating complex itself.[1]

The dimers **P** and **B** become brightly luminescent when intercalated between the base pairs of DNA,[6] similar to the parent “molecular light-switch” complex, $[\text{Ru}(\text{L})_2\text{dppz}]^{2+}$ (dppz=dipyrido[3,2-*a*:2',3'-*c*]phenazine).[7, 8] In polypyridyl ruthenium(II) complexes, luminescence takes place from a charge-separated excited state of triplet character (metal to ligand charge transfer, MLCT).[9] For $[\text{Ru}(\text{phen})_2\text{dppz}]^{2+}$, the dppz ligand has the lowest lying π^* -orbital, and the charge transfer electron is after excitation localised to the dppz moiety.[10, 11] The “light-switch” effect is due to protection of the phenazine nitrogens of the dppz ligands from hydrogen bonding to water when intercalated between the DNA base

pairs.[7, 12] The increase in emission quantum yield when bound to DNA is several orders of magnitude compared to in water and makes luminescence a sensitive tool to study DNA binding of these complexes. Thus, the quantum yield and the excited state lifetime of the monomer $[\text{Ru}(\text{phen})_2\text{dppz}]^{2+}$ and the dimers **B** and **P** when bound to DNA probe the accessibility of the phenazine moiety to water, which is found to vary significantly depending on the chirality of the ruthenium centre and the DNA sequence.[6, 8, 13]

While the quantum yield, luminescence lifetimes and emission spectra are similar for $\Delta\Delta\text{-B}$ and $\Delta\Delta\text{-P}$ (Δ denoting the propeller-like ruthenium coordination to be right handed, Λ left handed) when intercalated into mixed sequence calf thymus DNA (ct-DNA), the emission is significantly red-shifted with little change in quantum yield for $\Delta\Delta\text{-B}$, while, on the contrary, the emission is five times more intense and slightly blue-shifted for $\Delta\Delta\text{-P}$ when bound to poly(dAdT)₂. Taking advantage of the differences in emission properties of $\Delta\Delta\text{-B}$ and $\Delta\Delta\text{-P}$ when bound to ctDNA and poly(dAdT)₂ we have earlier established the thermodynamic preference of the binuclear complexes for the latter DNA,[1] and also determined the intrinsic dissociation rates and characterised the thermodynamics of the threading intercalation equilibrium for ct-DNA. (Westerlund et. al., manuscript)

In the present work, we examine the structural origin of these different effects on the photophysics by studying steady state and time resolved luminescence of $\Delta\Delta\text{-B}$ and $\Delta\Delta\text{-P}$ bound to hairpin oligonucleotides of varying AT-content and compare with the complexes bound to poly(dAdT)₂ and ct-DNA. We show that the emission quantum yield for $\Delta\Delta\text{-P}$ increases with increasing length of the central AT-tract of the oligonucleotide but that not even four complete helix-turns of AT-base pairs is enough to mimic the high quantum yield when bound to poly(dAdT)₂ completely. $\Delta\Delta\text{-B}$ on the other hand has a similar emission quantum yield for the two DNAs and for the oligonucleotides with long AT-tracts (including poly(dAdT)₂ but the AT-rich sequences show a significant red-shift in the emission maximum

(up to 50 nm). We ascribe the different behaviour to that the two complexes adapt to the increased flexibility of long AT-tracts[14] in opposite ways: whereas $\Delta\Delta\text{-P}$ hides its azanitrogens from quenching by water, $\Delta\Delta\text{-B}$ exposes them.

ACCEPTED MANUSCRIPT

Experimental

Chemicals

Experiments were conducted in 150 mM NaCl aqueous buffer (1 mM cacodylate, pH 7.0). Highly polymerised type I sodium salt calf thymus DNA, obtained from Sigma, was dissolved in buffer and filtered three times through a 0.8 μm Millipore filter before use. Sodium salt of polynucleotide poly(dAdT)₂, obtained from Amersham Biosciences, was dissolved in buffer and used without further purification. The concentration of DNA nucleobases were estimated using extinction coefficients of 6600 $\text{M}^{-1}\text{cm}^{-1}$ at 260 nm for calf thymus DNA and 262 nm for poly(dAdT)₂. HEG-linked oligonucleotides, obtained from ATDbio Ltd. (UK), were dissolved in buffer and re-annealed (90-5°C, 0.25°C/min) before use. Extinction coefficients were calculated using software available at <http://www.ambion.com>. The sequence of the oligonucleotides are: 5'-CCGGXGGCC-HEG-GGCCXCCGG-3', where HEG = hexaethylene glycol. Two different oligonucleotide series are studied. In the first series (denoted *AT*) the variable middle sequence (**X**) is an increasing number of consecutive AT base pairs from (AT)₅ (10 consecutive AT base pairs) to (AT)₂₂ (44 consecutive base pairs). In the second series (denoted *mix*) the middle sequence is varied according to Table 1. Metal complexes were synthesised as described elsewhere[3, 8] and concentrations were estimated spectrophotometrically using extinction coefficients at 412 nm of 65 000 $\text{M}^{-1}\text{cm}^{-1}$ and 75 800 $\text{M}^{-1}\text{cm}^{-1}$ for **B** and **P**, respectively.

Table 1

Sample preparation. Samples were prepared by mixing ruthenium complex and DNA/oligonucleotides dissolved in buffer and the samples were thereafter heated for 24 hours at 50°C. Ru-complex concentrations were 1 μM . Poly(dAdT)₂ and ct-DNA concentrations were, unless otherwise stated, 36 μM bases. Oligonucleotide concentrations were, unless

otherwise stated, 1 μM . Concentrations were determined using a Varian Cary 4B spectrophotometer.

Steady-state luminescence. Emission spectra were recorded on a xenon lamp equipped SPEX Fluorolog τ -3 Spectrofluorimeter (JY Horiba) using the S-channel. The samples were excited at 415 nm and emission measured between 500 and 850 nm.

Transient emission measurements. Emission lifetime measurements were performed on a setup where the exciting light is provided by a pulsed Nd:YAG laser (Continuum Surelite II-10, pulse width <7 ns) pumping an OPO (optical parametric oscillator) giving a tuneable excitation wavelength of 400-700 nm. The emitted light is collected at an angle of 90 degrees relative to the excitation light and, after passing a monochromator, detected by a five stage Hamamatsu R928 photomultiplier tube. The decays are collected and averaged by a 200 MHz digital Oscilloscope (Tektronix TDS2200 2Gs/s) and stored by a LabView-program (developed at the department), which controls the instrument setup. The oscilloscope is triggered by a photodiode that detects the exciting laser pulse. In the experiments an excitation wavelength of 440 nm was used and the emission decays were probed at 620 nm. In general, 32 measurements were averaged for each sample. The energy of the exciting laser was kept below 20 mJ/pulse to prevent photo-degradation of the samples.

Results

The emission spectra of $\Delta\Delta$ - $[\mu$ -bidppz(bipy) $_4$ Ru $_2$] $^{2+}$ and $\Delta\Delta$ - $[\mu$ -bidppz(phen) $_4$ Ru $_2$] $^{2+}$ (hereafter referred to as **B** and **P**, respectively) bound to ct-DNA and poly(dAdT) $_2$ are shown in Figure 2. Whereas the emission from **B** decreases slightly and the maximum is shifted 50 nm to the red when comparing complex bound to poly(dAdT) $_2$ with complex bound to ct-DNA, **P** has a five fold higher emission when bound to poly(dAdT) $_2$ and no significant shift in wavelength of maximum emission compared to complex bound to ct-DNA.

All emission decays of **B** and **P** bound to the two oligonucleotide series (*mix* and *AT*, sequences see Materials & Methods and Table 1), poly(dAdT) $_2$ and ct-DNA could be fitted satisfactorily with a sum of two individual exponentials. Lifetimes τ_i , and pre-exponential factors α_i , from bi-exponential fits to the decays of **P** and **B** bound to the oligonucleotides in the *AT*-series and poly(dAdT) $_2$, are shown in Table 2 and Figure 3. Both emission lifetimes increase with increasing length of the AT-tract for **P**, whereas the α -values are more or less constant over the series. On the contrary, for **B**, the longer lifetime tends to decrease and its α -value to increase with increasing length of the AT-tract, however, there are more individual deviations from the trend than for **P**.

Table 2

Table 2 also gives the corresponding emission quantum yields for **B** and **P**, which are plotted against AT-content in Figure 4 (top panel). The emission quantum yield increases with the number of consecutive AT base pairs for **P**, but it varies comparably little with sequence for **B**. When bound to the oligonucleotide with ten consecutive AT ((**AT**) $_5$)base pairs **P** has an emission quantum yield that is slightly higher than when bound to ct-DNA, however not even binding to the oligonucleotide with 44 consecutive AT base pairs ((**AT**) $_{22}$) gives an emission quantum yield for **P** that is as high as when bound to poly(dAdT) $_2$. Figure 4 (bottom panel) shows the average lifetime $\Sigma\alpha_i\tau_i$ for **B** and **P**. The trend for **P** is similar to the trend for

emission quantum yield, although the differences are less pronounced. The same is true when comparing average lifetime and emission quantum yield for **B**, but the variation in the average lifetime is even smaller than for **P**.

Table 3 gives τ_i and α_i from fits to the emission decays of **B** and **P** bound to the oligonucleotides in the *mix*-series and ct-DNA, as well as the corresponding emission quantum yields. In view of the opposite trends and lifetime differences for the two complexes found in the *AT*-series, the lifetimes and pre-exponential factors are surprisingly similar for **B** and **P** bound to ct-DNA and the oligonucleotides O2, O4 and O5. The emission quantum yields and average lifetimes of the same systems are plotted in Figure 5. The quantum yield is higher for **P** bound to ct-DNA than in all oligonucleotides in the *mix*-series except the one with ten consecutive base pairs, even though stretches of more than six AT base pairs are statistically very rare in ct-DNA. However, the quantum yield is larger for two stretches of four AT base pairs (O2) than for six consecutive AT base pairs (O3), suggesting that it is not only the number of consecutive AT base pairs that are decisive for the magnitude of the emission quantum yield. This conclusion is further supported by the observation that three sites with two AT base pairs (O4) gives a significantly higher quantum yield than two sites with three AT base pairs (O5). The difference is even larger when comparing three (O4) and two (O6) sites with two AT base pairs each.

Table 3

The trends in emission quantum yields in the *mix*-series are different for **B** compared to **P**; they are lower for all oligonucleotides than for ct-DNA, and two oligonucleotides stand out with very low quantum yields: O3, the oligonucleotide with six consecutive AT base pairs, and O6, the oligonucleotide with two sites with two AT base pairs. However, the average lifetimes follow very closely the same values as for **P** with the exception of O2, O6 and O1.

Interestingly, **B** has a higher emission quantum yield when bound to ct-DNA than when bound to any of the oligonucleotide sequences in both series.

Figure 6 (top panel) shows **B** bound to ct-DNA compared with oligonucleotide O4 (left) and **B** bound to poly(dAdT)₂ compared with oligonucleotide (AT)₂₂ (right). Even though the emission quantum yield is lower for O4 than ct-DNA, the spectral shape is very similar. For **B** bound to poly(dAdT)₂ and (AT)₂₂ the emission spectra are similar in both shape and intensity. The change in spectral shape for **B** when the AT-content increases is analysed by a least square projection of the spectra of the *mix*- and the *AT*-series onto the space spanned by the spectra of **B** bound to ct-DNA and poly(dAdT)₂ (bottom panel). It was found that all spectra (*S*) could be satisfactorily expressed as $S = c_1 S_{\text{ctDNA}} + c_2 S_{\text{AT}}$, and the coefficients (*c*₁ and *c*₂) are plotted versus length of the AT-tracts in Figure 6 (the two oligonucleotides with very low emission quantum yields, O3 and O6, were left out). Interestingly, there is an almost monotonic increase in the poly(dAdT)₂ coefficient with increasing number of AT-base pairs, despite the somewhat fluctuating quantum yields in the series. Since the ct-DNA coefficient varies less, a gradual red-shift in the spectra is thus a consequence of the increasing ratio of the poly(dAdT)₂ to the ct-DNA coefficients (*c*₂/*c*₁).

Discussion

The emission spectra and emission intensity for **B** and **P** are relatively similar when bound to ct-DNA, but when they are bound to poly(dAdT)₂ the difference is striking (Figure 2). For this kind of ruthenium complexes, the emission intensity and the excited state lifetimes when bound to DNA are related to the accessibility of the phenazine nitrogens of the bridging ligand to water. This indicates that **B** and **P** have a quite similar binding geometry when intercalated into ct-DNA and into the three oligonucleotides in the *mix*-series with the most AT/GC mixed sequences (O2, O4 and O5), but when they are intercalated into poly(dAdT)₂ and the oligonucleotides with the long AT-tracts, the accessibility to quenching by water is very different for the two complexes. Assuming mixed sequenced DNA to be more rigid, the two complexes thus, from a common starting point, take advantage of the increasing flexibility of the central AT-tract[14] in opposite ways: **B** exposes its phenazine nitrogens to quenching by water to a larger extent than when bound to ct-DNA whereas **P** hides them.

Comparing the complexes bound to the oligonucleotides with short AT-tracts (2-6 consecutive AT base pairs) shows that it is not only the length of the AT-tract that is important for the photophysical properties, but also how far apart the AT-sites are. This is most clearly seen when comparing the oligonucleotides with two and three sites with two consecutive AT base pairs (O4 and O6). For **B** bound to O3 and O6 the emission quantum yield is almost zero, while **P** has a relatively high quantum yield when bound to O3 and a low when bound to O6. There are on the other hand oligonucleotides, O4 and O5, where **B** is more luminescent than **P**, despite the fact that the average lifetimes are similar. These observations of discrepancies in the proportionality between the average lifetime and the quantum yield suggest that the complexes have binding sites on the oligonucleotides characterised by high affinity but almost completely quenched luminescence. Since **P** has a very low quantum yield

when threading intercalated into poly(dGdC)₂,[3] one possible location of such a binding site is close to the GC rich ends of the oligonucleotides.

Two discrete lifetimes are necessary to model the excited state decays of both **B** and **P** bound to all nucleic acids studied here, and the decays cannot be simulated satisfactorily by a distribution model with a single maximum. The situation is similar to the parent monomer, Δ -[Ru(phen)₂dppz]²⁺, which also shows two lifetimes with almost any DNA sequence studied.[13] The most simple interpretation of the two emission lifetimes is to assign them to two, structurally distinct (on the microsecond timescale), luminescent species for each complex, for which the water quenching rates are functions of the conformation of the nucleic acid and the structure of the complex. For both **B** and **P**, the specie corresponding to the long lifetime will dominate the shape of the emission spectrum since it has a fractional contribution which, with few exceptions, is over 85%. Many different structural distinctions could be envisaged that account for the two species: perpendicular or side-on intercalation from the major groove,[15] intercalation from the minor or major groove,[16] threading in-between either the pApT or the pTpA base pair step in the alternating central sequence, [17] inter-complex interactions[13] or different populations of bound water molecules close to the phenazine nitrogens. However, for the following discussion, we do not need to specify the nature of the structural distinction, although some explanations may turn out to be more plausible than others.

Analysis of spectral and photophysical data of the stereoisomers of **P** intercalated into different DNA-sequences have indicated that the intercalation into DNA is unsymmetrical, and that one of the [Ru(phen)₂dppz]²⁺-subunits is more deeply intercalated, presumably from the minor groove.[3] In a photophysical study of **P** and a rigid, planar homologue we have recently suggested that upon intercalation, the charge transfer in **P** will essentially be localised to the deeply intercalated [Ru(phen)₂dppz]²⁺-subunit.[6] Thus, in analogy with the parent

mononuclear $[\text{Ru}(\text{phen})_2\text{dppz}]^{2+}$, we may assign a specie with long lifetime and 630 nm emission to a completely water-protected species **b**, a short-lived red-shifted emission to a specie **c** that has received one hydrogen bond in the excited state, and an almost completely quenched emission to a specie **d**. [18]

A decrease in emission quantum yield and lifetime, but small spectral shift, can be expected when the first hydrogen bonding step is rate-limiting (**b** \rightarrow **c**), suggesting that this is the quenching mechanism of the long lifetime for **P** in the *AT*-series. A decrease in quantum yield and lifetime and a gradually red-shifted spectrum can be expected when both nitrogens are accessible for hydrogen bonding at comparable rates (**b** \rightarrow **c** \rightarrow **d**), consistent with the quenching process of the long lifetime for **B** in the *AT*-series.

What is the cause of the different accessibility to quenching by water of **B** and **P** in the *AT*-series? One explanation could be complex-complex interactions mediated by the middle ring of the phenanthroline. We have earlier reported that **P** has a tendency to bind in a more cooperative way in the thermodynamic equilibrium distribution on DNA that slowly forms from the initially distribution of threaded complexes, a process that is accompanied by an increase in emission quantum yield. [4] If complex-complex interactions were important for the photophysical properties of **P**, we would have expected an effect from variations in binding density, as observed for the parent monomer. [8, 13] However, varying the ratio from 1 to 3 complexes per oligonucleotide in the *AT*-series and from $\text{P/Ru}=18$ to $\text{P/Ru}=52$ in $\text{poly}(\text{dAdT})_2$, gave variations in lifetimes and pre-exponential factors of less than 5% (data not shown).

When inter-complex interactions are ruled out as less plausible explanations, we are left with models based on interactions of an isolated complex with the nucleic acid. A rotation around the helix axis of the complex in the intercalation pocket, as originally proposed by J. K. Barton and co-workers [15] for the parent mononuclear complex, could very well account for

the differences in quenching efficiency. Further structural degrees of freedom that could affect the water accessibility of the phenazine nitrogens could be symmetrical vs minor or major groove biased threading, as well as the bidppz conformation being *anti* or *syn*. Since the *meso*-form of **P** intercalated into poly(dAdT)₂ has the emission characteristics of the $\Lambda\Lambda$ -enantiomer, a phenanthroline of the non-intercalated Δ -[Ru(phen)₂dppz]²⁺-part was concluded to make a stabilising contact with the major groove.[3] If such an interaction has a steric or hydrophobic component involving the middle phenanthroline ring, a different interaction would be made by the bipyridine of **B**, which might instead favour a close distance to a phosphate group as the rigidity of the B-DNA structure is decreased in the AT-stretch.

The results obtained in this study are also of significance in a wider context, namely regarding the kinetic selectivity of these complexes for AT-rich DNA.[1] We have earlier ascribed the kinetic selectivity mainly to that the larger flexibility of AT-DNA will lower the activation free energy barrier. This study shows that the gradual decrease of the barrier with increasing length of the AT-tract is paralleled by a gradual change in the equilibrium properties of the intercalated state demonstrated by the change in water quenching efficiency. Thus, our results indicate that, by allowing the nucleic acid to adapt more readily to the semirigid structure of the complexes, the larger flexibility of long AT-tracts can lower both the transition state and the equilibrium binding free energies.

Conclusions

From studying the emission properties of **B** and **P** bound to oligonucleotides with varying AT-content, ct-DNA and poly(dAdT)₂ the following has been learnt:

- Two excited state lifetimes are needed to fit the emission decays for **B** and **P** when bound to all oligonucleotides as well as ct-DNA and poly(dAdT)₂, similarly to the monomer [Ru(phen)₂dppz]²⁺.
- The luminescence properties are similar for **B** and **P** when bound to ct-DNA but as the length of the central AT-tract of the oligonucleotides is increased, the emission quantum yield and lifetimes are decreased for **B** and increased for **P**. However, we cannot, even with four helix turns of AT base pairs, mimic the high quantum yield of **P** bound to poly(dAdT)₂.
- Ruling out other causes, this observation suggests that an increase in flexibility of the AT-rich double helix is exploited in opposite ways by the two complexes: the biddpz ligand of **B** gets more and that of **P** less exposed to quenching by water.

References

1. Nordell, P., Westerlund, F., Wilhelmsson, L.M., Nordén, B., and Lincoln, P. (2007). Kinetic Recognition of AT-Rich DNA by Ruthenium Complexes. *Angew. Chem., Int. Ed.* *46*, 2203-2206.
2. Wilhelmsson, L.M., Westerlund, F., Lincoln, P., and Nordén, B. (2002). DNA-Binding of Semirigid Binuclear Ruthenium Complex Δ,Δ - $[\mu$ -(11,11'-bidppz)(phen) $_4$ Ru $_2$] $^{4+}$: Extremely Slow Intercalation Kinetics. *J. Am. Chem. Soc.* *124*, 12092-12093.
3. Wilhelmsson, L.M., Esbjörner, E.K., Westerlund, F., Nordén, B., and Lincoln, P. (2003). Meso Stereoisomer as a Probe of Enantioselective Threading Intercalation of Semirigid Ruthenium Complex $[\mu$ -(11,11'-bidppz)(phen) $_4$ Ru $_2$] $^{4+}$. *J. Phys. Chem. B* *107*, 11784-11793.
4. Westerlund, F., Wilhelmsson, L.M., Nordén, B., and Lincoln, P. (2005). Monitoring the DNA Binding Kinetics of a Binuclear Ruthenium Complex by Energy Transfer: Evidence for Slow Shuffling. *J. Phys. Chem. B* *109*, 21140-21144.
5. Nordell, P., and Lincoln, P. (2005). Mechanism of DNA threading intercalation of binuclear ru complexes: uni- or bimolecular pathways depending on ligand structure and binding density. *J. Am. Chem. Soc.* *127*, 9670-9671.
6. Westerlund, F., Eng, M.P., Winters, M.U., and Lincoln, P. (2007). Binding Geometry and Photophysical Properties of DNA-Threading Binuclear Ruthenium Complexes. *J. Phys. Chem. B* *111*, 310-317.
7. Friedman, A.E., Chambron, J.C., Sauvage, J.P., Turro, N.J., and Barton, J.K. (1990). A molecular light switch for DNA: Ru(bpy) $_2$ (dppz) $^{2+}$. *J. Am. Chem. Soc.* *112*, 4960-4962.

8. Hiort, C., Lincoln, P., and Nordén, B. (1993). DNA-Binding of Delta- $[\text{Ru}(\text{Phen})_2\text{dppz}]^{2+}$ and Lambda- $[\text{Ru}(\text{Phen})_2\text{dppz}]^{2+}$. *J. Am. Chem. Soc.* *115*, 3448-3454.
9. Krausz, E., and Ferguson, J. (1989). The spectroscopy of the tris(bipyridine)ruthenium(2+) system. *Prog. Inorg. Chem.* *37*, 293-390.
10. Chambron, J.C., Sauvage, J.P., Amouyal, E., and Koffi, P. (1985). $\text{Ru}(\text{bipy})_2(\text{dipyridophenazine})^{2+}$: a complex with a long range directed charge transfer excited state. *Nouveau Journal de Chimie* *9*, 527-529.
11. Önfelt, B., Olofsson, J., Lincoln, P., and Nordén, B. (2003). Picosecond and Steady-State Emission of $[\text{Ru}(\text{phen})_2\text{dppz}]^{2+}$ in Glycerol: Anomalous Temperature Dependence. *J. Phys. Chem. A* *107*, 1000-1009.
12. Olofsson, J., Wilhelmsson, L.M., and Lincoln, P. (2004). Effects of Methyl Substitution on Radiative and Solvent Quenching Rate Constants of $[\text{Ru}(\text{phen})_2\text{dppz}]^{2+}$ in Polyol Solvents and Bound to DNA. *J. Am. Chem. Soc.* *126*, 15458-15465.
13. Tuite, E., Lincoln, P., and Nordén, B. (1997). Photophysical evidence that Delta- and Lambda- $[\text{Ru}(\text{phen})_2(\text{dppz})]^{2+}$ intercalate DNA from the minor groove. *J. Am. Chem. Soc.* *119*, 239-240.
14. Maltseva, T.V., Foldesi, A., Ossipov, D., and Chattopadhyaya, J. (2000). Comparative ^{13}C and ^2H relaxation study of microsecond dynamics of the AT tract of selectively $^{13}\text{C}/^2\text{H}$ double-labelled DNA duplexes. *Magn. Reson. Chem.* *38*, 403-414.
15. Hartshorn, R.M., and Barton, J.K. (1992). Novel dipyridophenazine complexes of ruthenium(II): exploring luminescent reporters of DNA. *J. Am. Chem. Soc.* *114*, 5919-5925.

16. Yun, B.H., Kim, J.-O., Lee, B.W., Lincoln, P., Nordén, B., Kim, J.-M., and Kim, S.K. (2003). Simultaneous Binding of Ruthenium(II) [(1,10-Phenanthroline)₂dipyridophenazine]²⁺ and Minor Groove Binder 4',6-Diamidino-2-phenylindole to Poly[d(A-T)₂] at High Binding Densities: Observation of Fluorescence Resonance Energy Transfer Across the DNA Stem. *J. Phys. Chem. B* *107*, 9858-9864.
17. Goodsell, D.S., Kaczor-Grzeskowiak, M., and Dickerson, R.E. (1994). The crystal structure of C-C-A-T-T-A-A-T-G-G. Implications for bending of B-DNA at T-A steps. *J. Mol. Biol.* *239*, 79-96.
18. Olofsson, J., Önfelt, B., and Lincoln, P. (2004). Three-State Light Switch of [Ru(phen)₂dppz]²⁺: Distinct Excited-State Species with Two, One, or No Hydrogen Bonds from Solvent. *J. Phys. Chem. A* *108*, 4391-4398.

Figure Legends

Figure 1 $[\mu\text{-bidppz(L)}_4\text{Ru}_2]^{4+}$ Top: **B** L=bipy. Bottom: **P** L=phen.

Figure 2 Emission from **B** (left panel) and **P** (right panel) bound to CT-DNA (solid) and poly(dAdT)₂ (dashed) in its final binding mode. The spectra have been normalised to the intensity for **P** bound to poly(dAdT)₂.

Figure 3 Parameters τ_i (left panels) and α_i (right panels), for fitting of the decays for **B** (top panels) and **P** (bottom panels) bound to the AT-series and poly(dAdT)₂. τ_1 and α_1 in white and τ_2 and α_2 in black.

Figure 4 Emission quantum yield (top panel) and $\Sigma\alpha_i\tau_i$ (bottom panel) for **B** (white) and **P** (black) bound to oligonucleotides of increasing length of the central AT-tract and to poly(dAdT)₂. The tract length varies from 10 ((AT)₅) to 44 ((AT)₂₂) consecutive AT base pairs. (AT)_n=poly(dAdT)₂.

Figure 5 Emission quantum yield (top) and $\Sigma\alpha_i\tau_i$ (bottom) for **B** (white) and **P** (black) bound to oligonucleotides (O1-O6) with sequences with indicated numbers of AT (white) and GC (gray) base pairs and ct-DNA.

Figure 6 Top panel: normalised spectra for **B** bound to ct-DNA (left section, thick line), oligonucleotide O4 (left section, thin line), poly(dAdT)₂, (right section, thick line) and oligonucleotide (AT)₂₂ (right section, thin line). Each panel has been normalised individually. Bottom panel: Coefficients from the projection (in the least square sense) of the spectra of oligonucleotide-bound **B** onto the space spanned by the ct-DNA and poly(dAdT)₂ spectra shown in the top panel.

Table 1 Oligonucleotide sequences for *mix*-series, CCGGXCCGG

	X=
O1	TATATATATA
O2	TATAGCTATA
O3	TATATA
O4	TAGCTAGCTA
O5	TATGGCCTAT
O6	TAGGCCGGTA

Table 2 Parameters τ_i and α_i from the fit of the decays of B and P in the AT-series (CCGGXCCGG) and poly(dAdT)₂ ((AT)_n) to two exponentials and the emission quantum yields (Φ).

X=	B					P				
	τ_1	α_1	τ_2	α_2	Φ	τ_1	α_1	τ_2	α_2	Φ
	(ns)		(ns)		(%)	(ns)		(ns)		(%)
(AT) _n	25	0.27	108	0.73	1.31	85	0.38	604	0.61	9.0
(AT) ₂₂	31	0.35	126	0.65	1.39	81	0.34	424	0.66	5.1
(AT) ₁₆	14	0.34	116	0.66	1.46	74	0.38	408	0.62	4.6
(AT) ₁₁	37	0.41	147	0.59	1.09	55	0.37	356	0.63	3.4
(AT) ₉	25	0.43	144	0.57	0.71	50	0.38	352	0.62	3.2
(AT) ₇	25	0.41	131	0.59	0.94	52	0.41	350	0.59	3.0
(AT) ₅	29	0.46	137	0.54	0.81	45	0.38	300	0.62	2.5

Table 3 Parameters τ_i and α_i from the fit of the decays of B and P in the *mix*-series and ct-DNA to two exponentials and the emission quantum yields (Φ).

	B					P				
	τ_1 (ns)	α_1	τ_2 (ns)	α_2	Φ (%)	τ_1 (ns)	α_1	τ_2 (ns)	α_2	Φ (%)
O2	52	0.64	303	0.36	0.87	50	0.51	273	0.49	1.21
O3	-	-	-	-	0.14	26	0.45	230	0.55	0.91
O4	54	0.61	404	0.39	0.48	61	0.66	432	0.34	0.62
O5	34	0.57	164	0.43	0.96	20	0.65	153	0.35	0.22
O6	-	-	-	-	0.11	24	0.77	217	0.23	0.19
Ct-DNA	38	0.55	227	0.45	1.64	40	0.51	264	0.49	2.1

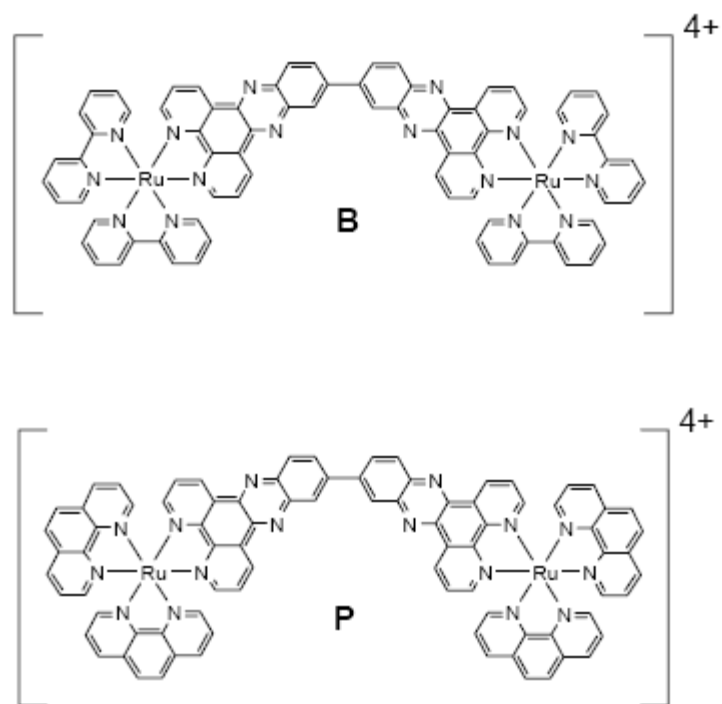


Figure 2

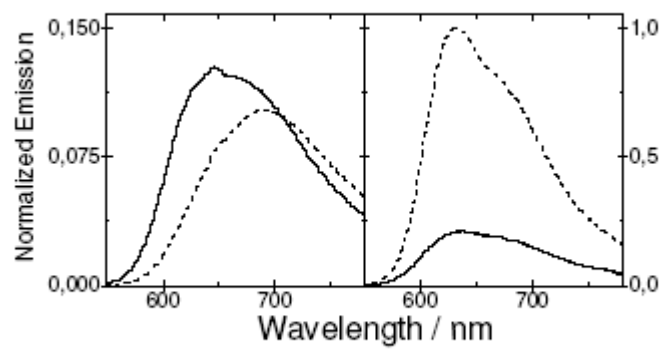


Figure 3

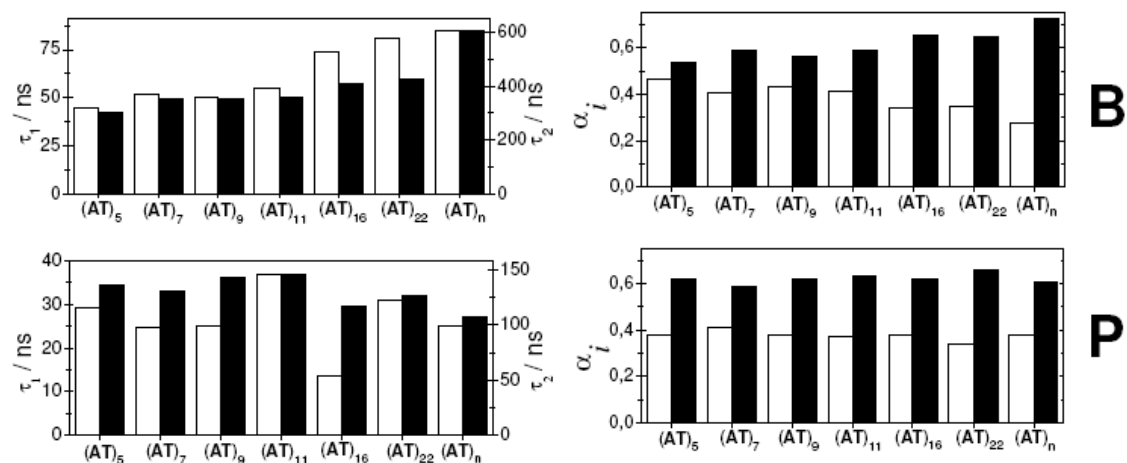


Figure 4

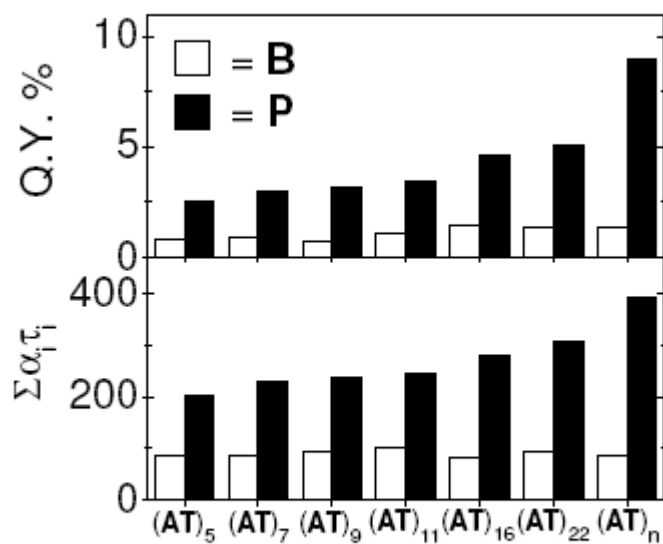


Figure 5

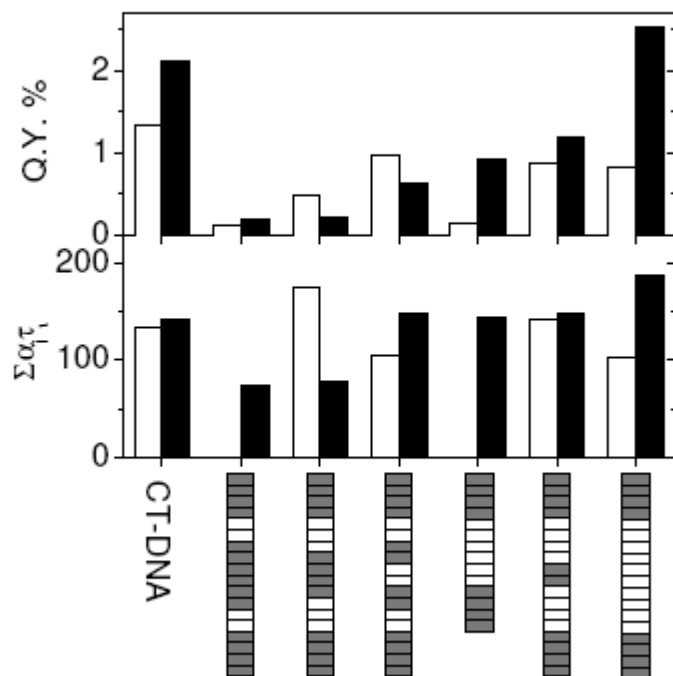
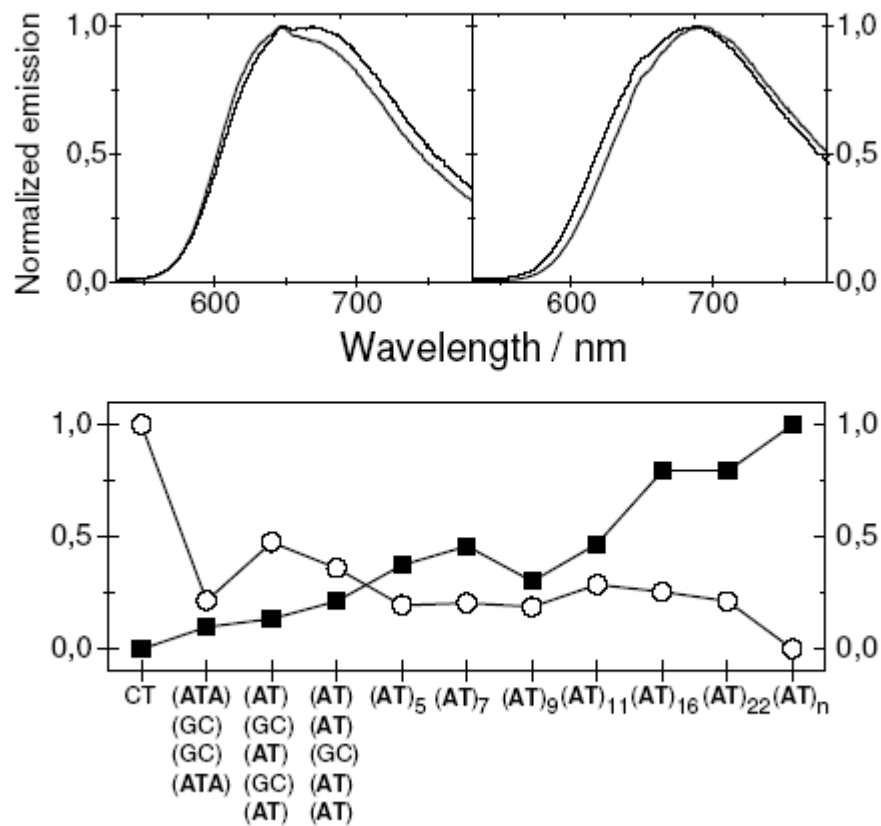


Figure 6



ACCEPT